Exclusive production of double light neutral mesons at the e^+e^- colliders

Junliang Lu,[1,2,*] Cai-Ping Jia,[3,2,†] Yu Jia,[2,4,‡] and Xiaonu Xiong[5,§]

[1]*School of Physics, Henan Normal University, Xinxiang 453007, China*
[2]*Institute of High Energy Physics, Chinese Academy of Sciences, Beijing 100049, China*
[3]*School of Nuclear Science and Technology, Lanzhou University, Lanzhou 730000, China*
[4]*School of Physics, University of Chinese Academy of Sciences, Beijing 100049, China*
[5]*School of Physics, Central South University, Changsha 410083, China*

(Received 10 January 2024; accepted 18 March 2024; published 13 May 2024)

In this work we investigate the exclusive production of a pair of light neutral mesons in e^+e^- annihilation, where the final state bears an even C-parity. The production processes can be initiated via the photon fragmentation or the nonfragmentation mechanism. While the fragmentation contribution can be rigorously accounted, the nonfragmentation contributions are calculated within the framework of collinear factorization, where only the leading-twist light-cone distribution amplitudes (LCDAs) of mesons are considered. Mediately solely by the nonfragmentation mechanism, the production rates of double light neutral pseudoscalar mesons are too small to be observed at the commissioning e^+e^- facilities. In contrast, the production rates of a pair of light neutral vector mesons are greatly amplified owing to the significant kinematic enhancement brought by the fragmentation mechanism. It is found that, at $\sqrt{s} = 3.77$ GeV, after including the destructive interference between the nonfragmentation and fragmentation contributions, the production rates for $e^+e^- \to \rho^0\rho^0$ and $\rho^0\omega$ can be lowered by about 10% and 30% relative to the fragmentation predictions. Future precise measurement of these exclusive double neutral vector meson production channels at BESIII experiment may provide useful constraints on the LCDAs of light vector mesons.

DOI: 10.1103/PhysRevD.109.094022

I. INTRODUCTION

The production of a pair of charged light mesons in e^+e^- annihilation, such as $e^+e^- \to \pi^+\pi^-, K^+K^-, \rho^+\rho^-, \cdots$, has been a widely studied topic from both experimental [1,2] and theoretical [3–7] perspectives. Since these processes proceed through the annihilation of e^+e^- into a virtual photon, the final-state mesons pair must carry the odd C-parity. These processes play a key role in determining the timelike electromagnetic form factors of charged mesons, from which one can infer their internal partonic structures.

On the other hand, exclusive production of double neutral mesons in e^+e^- annihilation, exemplified by $e^+e^- \to \pi^0\pi^0, K_SK_S, \pi^0\eta, \eta\eta', \rho^0\rho^0, \rho^0\omega, J/\psi J/\psi, J/\psi\rho^0, \cdots$, has also received considerable experimental and theoretical attention. Since the final-state mesons bear an even C-parity, these processes must proceed via the annihilation of e^+e^- into two virtual photons, then followed by the transition from $\gamma^*\gamma^*$ to two neutral mesons. One naturally expects the production rate for such processes to be much more suppressed with respect to that for production of a pair of charged mesons, due to the suppression brought by the extra powers of QED coupling constants. In 2009, Kivel and Polyakov have considered the exclusive production of double light pseudoscalar mesons in collinear factorization [8]. The cross section for $e^+e^- \to \pi^0\pi^0$ turns out to be several orders of magnitude smaller than that for $e^+e^- \to \pi^+\pi^-$.

In contrast to the $e^+e^- \to \pi^0\pi^0$ process, the exclusive production of double neutral vector mesons is more interesting from a theoretical angle. The $e^+e^- \to V_1V_2$ processes bear a distinct production mechanism: after annihilation of e^+e^- into two virtual photons, two virtual photons can independently fragment into two vector mesons. In the nonfragmentation mechanism, the valence quark and antiquark in each of the final-state mesons emerge from the splitting of two different virtual photons, thus the virtuality of each photon propagator is of order s. In contrast, the photon propagators in the two photon independent fragmentation processes carry a typical virtuality

*lujl@ihep.ac.cn
†jiacp@ihep.ac.cn
‡jiay@ihep.ac.cn
§xnxiong@csu.edu.cn

of order m_V^2, thus the fragmentation contribution is enhanced by powers of s/m_V^2 with respect to the nonfragmentation contribution. This kinematic enhancement factor may largely compensate for the suppression brought by extra powers of QED coupling α, so that there is a good chance to observe these processes at e^+e^- colliders. Actually in 2008 the *BABAR* Collaboration reported the first observation of the $e^+e^- \to \rho^0\rho^0$ and $\rho^0\phi$ processes [9]. Shortly after, only taking into account the photon fragmentation contribution, Davier *et al.* [10] and Bodwin *et al.* [11] already found satisfactory agreement between their theoretical prediction and the measured value.

Although not being observed experimentally, there has been extensive theoretical study for $e^+e^- \to VV$ when the vector meson is a vector charmonium such as J/ψ [11–14]. The nonfragmentation contribution can be accesses in the nonrelativistic QCD (NRQCD) approach [15]. It is found that at B factory, the interference between fragmentation and nonfragmentation amplitudes for double J/ψ production is destructive and non-negligible. For example, the leading-order NRQCD study indicates that including the interference effect can lower the fragmentation contribution to the cross section by 30% [13].

To the best of our knowledge, the nonfragmentation contribution to exclusive production of a pair of light neutral vector mesons has never been investigated in the literature. This might be largely due to the perfect agreement between the predictions from the photon fragmentation mechanism [10,11] and the *BABAR* measurements for $\rho^0\rho^0$ and $\rho^0\phi$ production rates [9], which implies that the nonfragmentation contribution might be safely neglected for double neutral light vector meson production at B factory energy. However, one may expect that the nonfragmentation mechanism might yield a non-negligible contribution for the double-ρ^0 production at BESIII energy, since the importance of the nonfragmentation contribution increases with the decreasing center-of-mass energy. Roughly speaking, since $(10.58\ \mathrm{GeV})^2/m_{J/\psi}^2 \approx (3.77\ \mathrm{GeV})^2/m_\rho^2$, the non-negligible nonfragmentation amplitude in $e^+e^- \to J/\psi J/\psi$ at B factory suggests that the nonfragmentation contribution to $e^+e^- \to \rho^0\rho^0$ at BESIII experiment may also be non-negligible.

The goal of this work is to make a comprehensive analysis of exclusive production of double light neutral vector mesons from e^+e^- annihilation, including both fragmentation and nonfragmentation contributions. We are especially interested in the BESIII energy, which seems to be sensitive to the interference effect induced by the nonfragmentation contribution. Following [8], we calculate the nonfragmentation amplitude in the framework of collinear factorization tailored for hard exclusive reactions [16,17]. For the sake of completeness, we also revisit the exclusive production of a pair of light neutral pseudoscalar mesons [8] and present a detailed phenomenological analysis. Our numerical studies indicate that the production rates for $e^+e^- \to \rho^0\rho^0, \rho^0\omega$ at $\sqrt{s} = 3.770$ GeV are large enough to be observed at the commissioning BESIII experiment. It is rewarding to measure the production rate of this exclusive production channel with high accuracy, so that one can clearly trace the footprint of the interference effect arising from the nonfragmentation mechanism. By confronting the future measurement with our predictions, there is a good chance to constraint the light-cone distribution amplitudes (LCDAs) of the ρ and ω meson, which might be useful for making more reliable predictions for the $B \to V$ form factor and $B \to VV$ processes.

The rest of this paper is distributed as follows. In Sec. II, we present the amplitude for exclusive production of double neutral vector mesons from e^+e^- annihilation, including both fragmentation and nonfragmentation parts. In Sec. III, we recap the amplitude for exclusive production of a pair light neutral pseudoscalars from e^+e^- annihilation, which are governed by the nonfragmentation mechanism only. The effect of η-η' mixing is also included. In Sec. IV, we present the analytic expressions of the polarized and unpolarized cross sections for $e^+e^- \to V_1^0 V_2^0$ and $e^+e^- \to P_1^0 P_2^0$. For the former, we also show the expressions of the interference and nonfragmentation parts. In Sec. V, we conduct a detailed numerical study for the angular distributions and the total cross sections for a variety of double neutral meson production processes at BESIII and Belle energies. We pay special attention to the $e^+e^- \to \rho^0\rho^0, \rho^0\omega$ channels at BESIII experiment, in which the destructive interference effect becomes non-negligible. It is advocated that the precise measurements of the angular distributions in these two channels may offer novel means to constrain the LCDAs of the ρ^0 and ω mesons. Finally we summarize in Sec. VI.

II. PRODUCTION AMPLITUDES OF $e^+e^- \to V_1^0 V_2^0$

We assume the e^+e^- center-of-mass energy $\sqrt{s}$ is high enough to warrant the applicability of perturbative QCD. At the lowest order in QED and QCD coupling constants, there arise four Feynman diagrams that contribute to $e^+e^- \to V_1^0 V_2^0$, which are depicted in Fig. 1. As stressed before, since the final-state mesons carry an overall even C parity, this process has to be mediated with two-photon exchange. Four Feynman diagrams can be categorized into the photon-fragmentation type (upper row) and photon nonfragmentation type (lower row).

In passing, we notice that our processes are similar, but much simpler than the high-energy production of double mesons in $\gamma\gamma$ fusion, which has been widely studied both experimentally [18–20] and theoretically [21–26]. The important difference is that, a hard gluon has to be exchanged between the outgoing quarks and antiquarks for the latter, while it is not necessary in our case, at least at the lowest order in α_s.

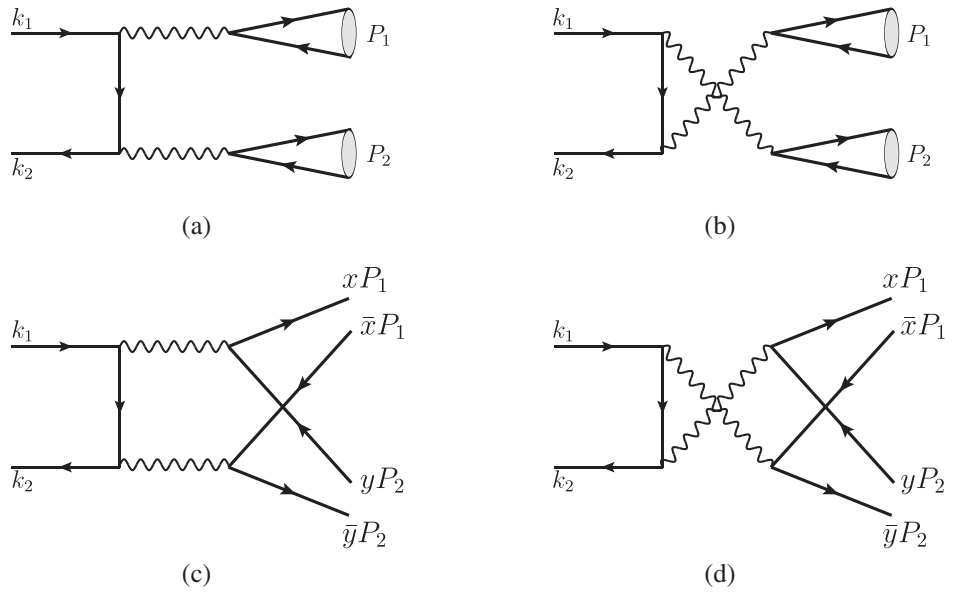

FIG. 1. The lowest-order Feynman diagrams for e^+e^- annihilation into two neutral mesons. The sub-figure (a) and (b) represents the photon fragmentation contribution, while the subfigure (c) and (d) represents the nonfragmentation contribution.

A. Photon fragmentation mechanism

As indicated in Figs. 1(a) and 1(b), two neutral mesons can be produced through two photon independent fragmentation mechanisms. Since the C-parity conservation forbids a photon to convert into a pseudoscalar meson, so we only need to consider the fragmentation production of two neutral vector mesons. Let us denote the momenta of the incoming e^- and e^+ by k_1 and k_2, and denote the momenta of the outgoing meson pairs by P_1 and P_2. The momenta are subject to the constraints $k_1^2 = k_2^2 = 0$, $k_1 \cdot k_2 = s/2$, and $P_i^2 = m_{V_i}^2$ $(i = 1, 2)$, where $\sqrt{s}$ signifies the center-of-mass energy, m_{V_i} indicating the mass of the ith neutral vector meson. The production amplitude from the two-photon independent fragmentation mechanism reads[1]

$$\begin{aligned}&\mathcal{A}^{\mathrm{fr}}(e^+e^- \to V_1^0(\lambda_1)V_2^0(\lambda_2)) \\ &= -\frac{e^2 g_{V_1} g_{V_2}}{m_{V_1}^2 m_{V_2}^2}\bar{v}(k_2)\left[\frac{\not{\epsilon}_2^*(\lambda_2)(\not{k}_1 - \not{P}_1)\not{\epsilon}_1^*(\lambda_1)}{(k_1 - P_1)^2}\right. \\ &\left. + \frac{\not{\epsilon}_1^*(\lambda_1)(\not{k}_1 - \not{P}_2)\not{\epsilon}_2^*(\lambda_2)}{(k_1 - P_2)^2}\right]u(k_1), \end{aligned} \tag{1}$$

where $\varepsilon_{1,2}$ signify the polarization vectors of two outgoing vector mesons, and g_V encodes the effective coupling between the photon and neutral vector meson [11]:

$$\langle V^0(P,\lambda)|j_{\mathrm{EM}}^{\mu}|0\rangle = g_V \epsilon^{(\lambda)\mu *}(P). \tag{2}$$

The electromagnetic current j_{EM}^{μ} can be decomposed into the isospin basis,

$$\begin{aligned} j_{\mathrm{EM}}^{\mu} &= e_u \bar{u}\gamma^{\mu}u + e_d \bar{d}\gamma^{\mu}d + e_s \bar{s}\gamma^{\mu}s + \cdots \\ &= \frac{e_u - e_d}{2}\bar{n}\tau^3\gamma^{\mu}n|_{I=1} + \frac{e_u + e_d}{2}\bar{n}\mathtt{1}\gamma^{\mu}n|_{I=0} \\ &\quad + e_s\bar{s}\gamma^{\mu}s|_{I=0} + \cdots, \end{aligned} \tag{3}$$

where $n = (u\ d)^T$ denotes the quark isospin doublet in the first generation, τ^3 and $\mathtt{1}$ signify the third Pauli matrix and the unit matrix in the isospin space. The subscripts in the second line of (3) are reminiscent of the isospin carried by various quark vector currents. $e_u = \frac{2}{3}$, $e_d = e_s = -\frac{1}{3}$ indicate the electric charges of the light quarks.

It is a common practice to work with the decay constant of a light neutral vector mesons, f_V. For three species of lowest-lying neutral vector mesons, the decay constants are defined via

$$\langle \rho^b(P,\lambda)|\bar{n}\tau^a\gamma_{\mu}n|0\rangle = \delta^{ab}\sqrt{2}f_{\rho}m_{\rho}\varepsilon_{\mu}^{(\lambda)*}(P), \quad (a,b=1,2,3) \tag{4a}$$

$$\langle \omega(P,\lambda)|\bar{n}\mathtt{1}\gamma_{\mu}n|0\rangle = \sqrt{2}f_{\omega}m_{\omega}\varepsilon_{\mu}^{(\lambda)*}(P), \tag{4b}$$

$$\langle \phi(P,\lambda)|\bar{s}\gamma_{\mu}s|0\rangle = f_{\phi}m_{\phi}\varepsilon_{\mu}^{(\lambda)*}(P), \tag{4c}$$

with ρ^3 identified with ρ^0 in (4a). m_V signifies the mass of the vector meson.

[1]Note that the photon-to-vector meson fragmentation mechanism is often referred to as the vector meson dominance (VMD) model [27] in literature (for example, see Ref. [10]). Nevertheless, in our process the vector mesons manifest themselves as the asymptotic out states, rather than appear in the intermediate state (vector meson propagator), therefore there is no model dependence in our treatment of the fragmentation amplitude.

The photon-to-V coupling g_V is related to the vector meson decay constant via

$$g_V = \mathcal{Q}_V f_V m_V \tag{5}$$

for $V = \rho^0, \omega, \phi$. Here $\mathcal{Q}_V$ characterizes the effective electric charge of quark affiliated with each neutral vector meson:

$$\mathcal{Q}_{\rho^0} = \frac{1}{\sqrt{2}}(e_u - e_d) = \frac{1}{\sqrt{2}},$$
$$\mathcal{Q}_\omega = \frac{1}{\sqrt{2}}(e_u + e_d) = \frac{1}{3\sqrt{2}}, \qquad \mathcal{Q}_\phi = e_s = -\frac{1}{3}. \tag{6}$$

The occurrence of the $\mathcal{Q}_V$ factor stems from the fact that the ρ^0 and ω mesons contain both u and d quarks in their flavor wave function, i.e., $\rho^0 = \frac{1}{\sqrt{2}}|u\bar{u} - d\bar{d}\rangle$, $\omega = \frac{1}{\sqrt{2}}|u\bar{u} + d\bar{d}\rangle$.

The leptonic width of the neutral vector meson then becomes

$$\Gamma(V^0 \to e^+e^-) = \frac{4\pi\alpha^2}{3}\frac{g_V^2}{m_V^3} = \frac{4\pi\mathcal{Q}_V^2\alpha^2}{3}\frac{f_V^2}{m_V}. \tag{7}$$

One thus can deduce the values of g_V and f_V from the precisely measured leptonic width.

B. Nonfragmentation contribution

The lowest-order nonfragmentation diagrams are depicted in Figs. 1(c) and 1(d), where the quark and antiquark in each outgoing vector meson stem from the splitting of two different photons. The photon propagators bear a typical virtuality of order s, much greater than m_V^2 in the fragmentation mechanism, therefore we expect such nonfragmentation contribution to be suppressed with respect to the fragmentation contribution. For a hard exclusive reaction involving hadrons, the amplitude can be expressed as a convolution between the perturbatively calculable hard scattering kernel and the nonperturbative yet universal LCDAs of hadrons. Following Ref. [8], we apply the collinear factorization to investigate the nonfragmentation contribution to $e^+e^- \to V_1^0 V_2^0$, at the lowest order in $1/s$ and α_s.

As the key input in collinear factorization, LCDAs characterize the momentum distribution of the valence quarks inside a fast-moving hadron. The LCDAs of a light vector mesons carrying helicity λ are related to the following quark correlator with lightlike separation through Fourier transform [28][2]:

$$\langle V(P,\lambda)|\bar{q}_\alpha(u_2)[u_2,u_1]q_\beta(u_1)|0\rangle = -\frac{i}{4}\int_0^1 dx e^{i(xp\cdot u_2 + \bar{x}p\cdot u_1)}\left\{f_V m_V \not{p}\frac{\varepsilon_\parallel^*\cdot u}{p\cdot u}\phi_\parallel(x) + f_\perp \not{\varepsilon}_\perp^* \not{p}\phi_\perp(x) + \cdots\right\}_{\beta\alpha}, \tag{8}$$

with $u \equiv u_1 - u_2$ and $u^2 = 0$. p_μ is a lightlike four-momentum which is related to the physical meson momentum P_μ via $p_\mu = P_\mu - m_V^2 u_\mu/(2P\cdot u)$. $\varepsilon_\parallel$ and $\varepsilon_\perp$ denote the polarization vector of the vector meson with helicity λ, and $\phi_\parallel(x)$ and $\phi_\perp(x)$ represent the leading-twist LCDAs for a longitudinally and transversely polarized vector meson, with x ($\bar{x} \equiv 1 - x$) signifying the light-cone momentum fraction carried by the quark (anti-quark). The ellipses represent all the neglected higher-twist contributions, which are irrelevant to our purpose. $[u_2, u_1]$ in (8) signifies the gauge link,

$$[u_2,u_1] = \mathcal{P}\left\{\exp\left[-ig_s\int_0^1 dt\, u_\mu A^\mu(tu_2 + (1-t)u_1)\right]\right\}, \tag{9}$$

which is inserted to ensure the gauge invariance of the LCDAs of a vector meson.

In addition to the usual decay constant f_V in (4), a new decay constant $f_{V\perp}$ also arises in (8), which is related to the transversely polarized vector meson:

$$\langle \rho^b(P,\lambda)|\bar{n}\tau^a\sigma_{\mu\nu}n|0\rangle = -\delta^{ab}\sqrt{2}f_{\rho\perp}(P_\mu\varepsilon_\nu^*(\lambda) - P_\nu\varepsilon_\mu^*(\lambda)), \quad (a,b=1,2,3) \tag{10a}$$

$$\langle \omega(P,\lambda)|\bar{n}1\sigma_{\mu\nu}n|0\rangle = -\sqrt{2}f_{\omega\perp}(P_\mu\varepsilon_\nu^*(\lambda) - P_\nu\varepsilon_\mu^*(\lambda)), \tag{10b}$$

$$\langle \phi(P,\lambda)|\bar{s}\sigma_{\mu\nu}s|0\rangle = -f_{\phi\perp}(P_\mu\varepsilon_\nu^*(\lambda) - P_\nu\varepsilon_\mu^*(\lambda)). \tag{10c}$$

To expedite computing the vector meson exclusive production amplitude, it is convenient to apply the light-cone projectors in the momentum space [28]:

$$M_{\beta\alpha}^V(x) = M_{\parallel\beta\alpha}^V(x) + M_{\perp\beta\alpha}^V(x), \tag{11}$$

where

$$M_\parallel^V(x) = -\frac{if_V}{4}\frac{m_V(\varepsilon^*\cdot n_+)}{2E}E\not{n}_-\phi_\parallel(x) + \cdots, \tag{12a}$$

[2]For simplicity, here we assume that V is a neutral vector meson made of a single flavor, e.g., the ϕ meson. The LCDAs of ρ^0 and ω can be obtained by inserting the matrices τ^3 or $\mathtt{1}$ in the isospin space.

$$M_{\perp}^{V}(x) = -\frac{if_{\perp}}{4} E \not{\varepsilon}_{\perp}^{*} \not{n}_{-} \phi_{\perp}(x) + \cdots \tag{12b}$$

are projectors for the longitudinally and transversely polarized vector meson, respectively. A pair of conjugate lightlike four-vectors $n_{\pm}$ are introduced through $P^{\mu} = En_{-}^{\mu} + m_V^2 n_{+}^{\mu}/(4E)$. Since we are not interested in the power-suppressed high-twist corrections, suffices it that to retain only the leading-twist LCDAs in (12), and it is legitimate to approximate the momentum of the vector meson by $P^{\mu} \approx p^{\mu} = En_{-}^{\mu}$.

Substituting (12) into the quark amplitude $e^+e^- \to q_1(xp_1)\bar{q}_1(yp_2) + q_2(\bar{y}p_2)\bar{q}_2(\bar{x}p_1)$, the nonfragmentation amplitudes of double neutral vector meson production can be obtained through

$$\mathcal{A}^{\rm nf}(e^+e^- \to V_1^0(\lambda_1)V_2^0(\lambda_2)) = e^4\kappa_{V_1V_2}\int\int dxdy \frac{\mathrm{Tr}[M_{\lambda_1}^{V_1}(y)\gamma^{\beta}M_{\lambda_2}^{V_2}(x)\gamma^{\alpha}]}{(xp_1+yp_2)^2(\bar{x}p_1+\bar{y}p_2)^2} \times \bar{v}(k_2)\left[\frac{\gamma_{\beta}(\not{k}_1 - x\not{p}_1 - y\not{p}_2)\gamma_{\alpha}}{(k_1 - xp_1 - yp_2)^2} + \frac{\gamma_{\alpha}(\not{k}_1 - \bar{x}\not{p}_1 - \bar{y}\not{p}_2)\gamma_{\beta}}{(k_1 - \bar{x}p_1 - \bar{y}p_2)^2}\right]u(k_1). \tag{13}$$

The factor $\kappa_{V_1V_2}$ represents the squared effective quark electric charge, which arises from the superposition of the quark amplitude in the flavor space. The concrete values of $\kappa_{V_1V_2}$ are tabulated in Table I.[3]

After some straightforward manipulation, we obtain the nonfragmentation amplitudes from various helicity configurations:

$$\mathcal{A}_{\pm1,\mp1}^{\rm nf} = \frac{e^4\kappa_{V_1V_2}f_{V_1\perp}f_{V_2\perp}}{N_c s^2}\bar{v}(k_2) \times [(\varepsilon_{1\perp}^{*}\cdot k_1)\not{\varepsilon}_{2\perp}^{*} + (\varepsilon_{2\perp}^{*}\cdot k_1)\not{\varepsilon}_{1\perp}^{*}] \times u(k_1)G_{\pm1,\mp1}(\cos\theta), \tag{14a}$$

$$\mathcal{A}_{0,0}^{\rm nf} = \frac{e^4\kappa_{V_1V_2}f_{V_1}f_{V_2}}{N_c s^2}\bar{v}(k_2)(\not{p}_1 - \not{p}_2)u(k_1)G_{0,0}(\cos\theta), \tag{14b}$$

$$\mathcal{A}_{\pm1,\pm1}^{\rm nf} = \mathcal{A}_{\pm1,0}^{\rm nf} = \mathcal{A}_{0,\mp1}^{\rm nf} = 0. \tag{14c}$$

where

$$G_{\pm1,\mp1}(z) = \int\int dxdy \frac{\phi_{1,\perp}(x)}{x\bar{x}}\frac{\phi_{2,\perp}(y)}{y\bar{y}} \times \frac{x+y-2xy}{(x+y-2xy)^2 - z^2(x-y)^2}, \tag{15a}$$

$$G_{0,0}(z) = z\int\int dxdy \frac{\phi_{1,\parallel}(x)}{x\bar{x}}\frac{\phi_{2,\parallel}(y)}{y\bar{y}} \times \frac{x\bar{x}+y\bar{y}}{(x+y-2xy)^2 - z^2(x-y)^2}. \tag{15b}$$

[3]Note we have omitted the small ρ^0-ω and ω-ϕ mixing effects for simplicity.

It is reassuring that the two-fold integration in $G(z)$ renders a finite result, provided that the leading-twist LCDAs assume the standard endpoint behavior: $\phi_{\parallel}(x) \sim \phi_{\perp}(x) \propto x$.

We also remark that, $\mathcal{A}_{0,0}^{\rm nf}$ in (14) is identical to the amplitude for producing double pseudoscalar mesons in (19), except the corresponding replacement with the leading-twist LCDA and the decay constant is made. This is not a coincidence, since the hard-scattering amplitude in collinear factorization is only sensitive to the meson helicity, rather than the meson's spin.

III. PRODUCTION AMPLITUDES OF $e^+e^- \to P_1^0P_2^0$

For the sake of completeness, in this section we recapitulate the calculation of exclusive production of a pair of light neutral pseudoscalar mesons from e^+e^- collision. We also consider the production channels involving $\eta(\eta')$ and K_S in addition to the $e^+e^- \to \pi^0\pi^0$ process investigated by Kivel and Polyakov [8]. Due to the mismatch of the quantum number between photon and pseudoscalar meson, the photon mechanism is absent in these processes, and we only need take into account the nonfragmentation contributions as indicated by Figs. 1(c) and 1(d).

Analogous to the LCDAs of a vector meson as introduced in (8), the leading-twist LCDA of a pseudoscalar

TABLE I. The squared effective quark charge for $e^-e^+ \to M_1M_2$ in the nonfragmentation amplitude.

Channel	$\kappa_{V_1V_2}$	Value	Channel	$\kappa_{P_1P_2}$	Value
$\rho^0\rho^0$	$\frac{1}{2}(e_u^2+e_d^2)$	$\frac{5}{18}$	$\pi^0\pi^0$	$\frac{1}{2}(e_u^2+e_d^2)$	$\frac{5}{18}$
$\rho^0\omega$	$\frac{1}{2}(e_u^2-e_d^2)$	$\frac{1}{6}$	$\pi^0\eta_q$	$\frac{1}{2}(e_u^2-e_d^2)$	$\frac{1}{6}$
$\omega\omega$	$\frac{1}{2}(e_u^2+e_d^2)$	$\frac{5}{18}$	$\eta_q\eta_q$	$\frac{1}{2}(e_u^2+e_d^2)$	$\frac{5}{18}$
$\phi\phi$	e_s^2	$\frac{1}{9}$	$\eta_s\eta_s$	e_s^2	$\frac{1}{9}$
			$K^0\bar{K}^0$	e_de_s	$\frac{1}{9}$

meson is related to following light-cone quark correlator through Fourier transform [28]

$$\langle P(P)|\bar{q}_\alpha(u_2)[u_2,u_1]q_\beta(u_1)|0\rangle = \frac{if_P}{4}\int_0^1 dx e^{i(xp\cdot u_2+\bar{x}p\cdot u_1)}\{\not{p}\gamma_5\phi(x)+\cdots\}_{\beta\alpha}, \quad (16)$$

where the notations are identical to (8). Since the pseudoscalar merely carries zero helicity, there arises only one leading-twist LCDA $\phi(x)$. f_P signifies the decay constant of a pseudoscalar meson, which is defined through

$$\langle \pi^b(P)|\bar{n}\tau^a\gamma^\mu\gamma_5 n|0\rangle = i\delta^{ab}\sqrt{2}f_\pi P^\mu, \qquad (a,b=1,2,3) \quad (17a)$$

$$\langle \eta_q(P)|\bar{n}1\gamma^\mu\gamma_5 n|0\rangle = i\sqrt{2}f_{\eta_q}P^\mu,$$
$$\langle \eta_s(P)|\bar{s}\gamma^\mu\gamma_5 s|0\rangle = if_{\eta_s}P^\mu, \quad (17b)$$

$$\langle K^0(P)|\bar{d}\gamma^\mu\gamma_5 s|0\rangle = if_K P^\mu. \quad (17c)$$

with π^3 identified with π^0 in (17a).

The light-cone projector in momentum space is particularly simple for a pseudoscalar [28]:

$$M^P_{\beta\alpha}(x) = \frac{if_P}{4}(\not{p}\gamma_5)_{\beta\alpha}\phi(x), \quad (18)$$

where $p^\mu = En^\mu_-$ is a lightlike momentum, the same as in (12).

Substituting (18) into the quark amplitude $e^+e^-\to q_1(xp_1)\bar{q}_1(yp_2)+q_2(\bar{y}p_2)\bar{q}_2(\bar{x}p_1)$, one then obtains the intended amplitude for $e^+e^-\to P_1^0P_2^0$. This can be achieved by simply replacing the light-cone projectors $M^V_{\parallel(\perp)}$ with M^P in (13), and the resulting amplitude is

$$\mathcal{A}(e^+e^-\to P_1^0P_2^0) = \frac{e^4\kappa_{P_1P_2}f_{P_1}f_{P_2}}{N_c s^2}\bar{v}(k_2)\times(\not{p}_1-\not{p}_2)u(k_1)G_{P,P}(\cos\theta), \quad (19)$$

with

$$G_{P,P}(z) = z\int\int dxdy\frac{\phi_1(x)}{x\bar{x}}\frac{\phi_2(y)}{y\bar{y}}\times\frac{x\bar{x}+y\bar{y}}{(x+y-2xy)^2-z^2(x-y)^2}. \quad (20)$$

These expressions are in agreement with (2.1) and (2.2) of Ref. [8]. Again the angular function $G_{P,P}(\cos\theta)$ is finite as long as $\phi_i(x)\propto x$ near the endpoint regime.

The factor $\kappa_{P_1P_2}$ in (19) has the same physical meaning as $\kappa_{V_1V_2}$ in (13). It represents the squared effective quark electric charge, which emerges from the superposition of the quark amplitude in the flavor space. The concrete values of various $\kappa_{P_1P_2}$ have been tabulated in Table I.

Some special care is needed when the final-state mesons involve η or η'. The pseudoscalar states appearing in (19) are actually not the physical η and η', but two isosinglets $\eta_q=(u\bar{u}+d\bar{d})/\sqrt{2}$ and $\eta_s=s\bar{s}$.[4] The physical η and η' states are the mixtures between η_q and η_s [29][5]:

$$\begin{pmatrix}\eta\\ \eta'\end{pmatrix} = \begin{pmatrix}\cos\phi & -\sin\phi\\ \sin\phi & \cos\phi\end{pmatrix}\begin{pmatrix}\eta_q\\ \eta_s\end{pmatrix}, \quad (21)$$

The mixing angle has been determined to be $\phi=(38.8\pm 2.4)^\circ$ [31].

Some explanation on the kaon pair exclusive production is in order. It is experimentally favorable to look for the $e^+e^-\to K_S^0K_S^0$ process. However, the kaon pair appearing in (19) are the flavor eigenstates K^0 and $\bar{K}^0$. Since the CP violation in neutral kaon is quite small, we can approximately assume $|K_S^0\rangle=\frac{1}{\sqrt{2}}(|K^0\rangle+|\bar{K}^0\rangle)$. Consequently, the amplitudes for $e^+e^-\to K_S^0K_S^0$ and $e^+e^-\to K^0\bar{K}^0$ turn out to be identical.

IV. DIFFERENTIAL CROSS SECTIONS FOR DOUBLE NEUTRAL MESON PRODUCTION

In the preceding sections we have obtained the amplitudes of exclusive neutral meson pair production, and it is straightforward to deduce the corresponding differential polarized cross sections:

$$\frac{d\sigma_{\lambda_1,\lambda_2}(e^+e^-\to M_1(\lambda_1)M_2(\lambda_2))}{d\cos\theta} = \frac{1}{2s}\frac{1}{16\pi}\frac{2|\mathbf{P}_1|}{\sqrt{s}}\frac{1}{4}\sum_{\text{spin}}|\mathcal{A}|^2, \quad (22)$$

where λ_i $(i=1,2)$ signifies the helicity of the ith meson in the final state, and the spins of electron and positron spin have been averaged over. θ represents the polar angle between the first meson's three-momentum and the moving direction of the electron beam. $|\mathbf{P}_1|$ denotes the magnitude of the meson three-momentum in the center-of-mass frame, $|\mathbf{P}_1|=\lambda^{\frac{1}{2}}(s,m_{V_1}^2,m_{V_2}^2)/(2\sqrt{s})$, with

$$\lambda(x,y,z)=x^2+y^2+z^2-2xy-2xz-2yz. \quad (23)$$

[4]Note that in order to predict $e^+e^-\to\pi^0\eta(\eta')$ production rate, we only need consider the amplitude of $e^+e^-\to\pi^0\eta_q$, since there arises no such reaction as $e^+e^-\to\pi^0\eta_s$ from the nonfragmentation mechanism.

[5]In literature there has been speculation that a pseudoscalar glueball may also mix with η and η' due to chiral anomaly [30]. Since the photon does not directly couple to gluon, we will not dwell on this complication for exclusive η and η' production.

A. Production rates for double neutral vector mesons

As elucidated in Sec. II, for double neutral vector meson production, both the fragmentation and nonfragmentation contributions have been considered. The differential cross sections can thus be decomposed into three pieces:

$$\begin{aligned}\frac{d\sigma_{\lambda_1,\lambda_2}(e^+e^-\to V_1^0(\lambda_1)V_2^0(\lambda_2))}{d\cos\theta}&=\frac{1}{2s}\frac{1}{16\pi}\frac{2|\mathbf{P}_1|}{\sqrt{s}}\frac{1}{4}\sum_{\text{spins}}|\mathcal{A}^{\text{fr}}+\mathcal{A}^{\text{nf}}|^2,\\&=\frac{d\sigma^{\text{fr}}_{\lambda_1,\lambda_2}}{d\cos\theta}+\frac{d\sigma^{\text{int}}_{\lambda_1,\lambda_2}}{d\cos\theta}+\frac{d\sigma^{\text{nf}}_{\lambda_1,\lambda_2}}{d\cos\theta}.\end{aligned}\tag{24}$$

At the commissioning e^+e^- collision experiments, the dominant contribution comes from the fragmentation part, and the next important contribution comes from the interference part. The nonfragmentation part is anticipated to yield a negligible contribution.

1. Fragmentation part

The photon fragmentation contribution to the polarized cross sections for double neutral vector meson production was first obtained by Bodwin *et al.* in 2006 [11]. We have confirmed the correctness of their expressions. Here for the sake of completeness, we enumerate the explicit expressions of the polarized cross section for all possible helicity configurations of the final-state vector mesons.

From (1) one can readily deduce the fragmentation contribution to the differential cross section for each helicity configurations (λ_1,λ_2) [11]:

$$\frac{d\sigma^{\text{fr}}_{\lambda_1,\lambda_2}}{d\cos\theta}=\frac{16\pi^3\alpha^4\mathcal{Q}^2_{V_1}\mathcal{Q}^2_{V_2}f^2_{V_1}f^2_{V_2}r^2_{V_1}r^2_{V_2}\lambda^{1/2}(1,r^2_{V_1},r^2_{V_2})F_{\lambda_1,\lambda_2}(r^2_{V_1},r^2_{V_2},\cos\theta)}{s^3r^4_{V_1}r^4_{V_2}[\lambda(1,r^2_{V_1},r^2_{V_2})\sin^2\theta+4r^2_{V_1}r^2_{V_2}]^2},\tag{25}$$

with the dimensionless ratios $r_{V_i}\equiv m_{V_i}/\sqrt{s}$ $(i=1,2)$. The helicity-dependent functions F_{λ_1,λ_2} read

$$F_{\pm1,\mp1}(r^2_{V_1},r^2_{V_2},z)=(1-z^4)(1-r^2_{V_1}-r^2_{V_2})^2,\tag{26a}$$

$$F_{\pm1,0}(r^2_{V_1},r^2_{V_2},z)=r^2_{V_2}[2r^4_{V_1}(z^4+6z^2+1)-4r^2_{V_1}(1-r^2_{V_2})(1-z^4)+2(1-r^2_{V_2})^2(z^2-1)^2],\tag{26b}$$

$$F_{0,\pm1}(r^2_{V_1},r^2_{V_2},z)=F_{\pm1,0}(r^2_{V_2},r^2_{V_1},z),\tag{26c}$$

$$\begin{aligned}F_{\pm1,\pm1}(r^2_{V_1},r^2_{V_2},z)=&\,4r^2_{V_1}r^2_{V_2}z^2(1-(r^2_{V_1}-r^2_{V_2})^2)-z^4(r^4_{V_1}+r^4_{V_2}\\&-r^2_{V_1}(2r^2_{V_2}+1)-r^2_{V_2})^2+(r^2_{V_1}-r^2_{V_2}-r^4_{V_1}+r^4_{V_2})^2,\end{aligned}\tag{26d}$$

$$F_{0,0}(r^2_{V_1},r^2_{V_2},z)=16r^2_{V_1}r^2_{V_2}z^2(1-z^2),\tag{26e}$$

The asymptotical behaviors of various polarized cross sections in (25) in the high energy limit are

$$\frac{d\sigma^{\text{fr}}_{\pm1,\mp1,}}{d\cos\theta}\sim\frac{\alpha^4}{s},\tag{27a}$$

$$\frac{d\sigma^{\text{fr}}_{\pm1,0}}{d\cos\theta}\sim\frac{d\sigma^{\text{fr}}_{0,\pm1}}{d\cos\theta}\sim\frac{\alpha^4\Lambda^2_{\text{QCD}}}{s^2},\tag{27b}$$

$$\frac{d\sigma^{\text{fr}}_{0,0}}{d\cos\theta}\sim\frac{d\sigma^{\text{fr}}_{\pm1,\mp1,}}{d\cos\theta}\sim\frac{\alpha^4\Lambda^4_{\text{QCD}}}{s^3},\tag{27c}$$

where we assume $f_V\sim m_{V_i}\sim\mathcal{O}(\Lambda_{\text{QCD}})$. It is the $(\pm1,\mp1)$ helicity channel that yields the most dominant contribution.

Summing (25) over all possible helicity configurations, we arrive at the fragmentation contribution to the unpolarized cross section:

$$\frac{d\sigma^{\text{fr}}(e^+e^-\to V_1^0V_2^0)}{d\cos\theta}=16\pi^3\alpha^4\left(\frac{\mathcal{Q}_{V_1}f_{V_1}}{m_{V_1}}\right)^2\left(\frac{\mathcal{Q}_{V_2}f_{V_2}}{m_{V_2}}\right)^2\lambda^{1/2}(1,r^2_{V_1},r^2_{V_2})\frac{2stu(m^2_{V_1}+m^2_{V_2})+(t^2+u^2)(tu-m^2_{V_1}m^2_{V_2})}{st^2u^2}\tag{28}$$

where the Mandelstam variables t, u are given by

$$t = -\frac{s}{2}\left(1 - 2r_{V_1}^2 - \sqrt{1-4r_{V_1}^2}\cos\theta\right),$$
$$u = -\frac{s}{2}\left(1 - 2r_{V_2}^2 + \sqrt{1-4r_{V_2}^2}\cos\theta\right). \quad (29)$$

Equation (28) is in agreement with what is found in Refs. [10,11].

2. Interference part

With the knowledge of the fragmentation amplitude in (1) and the nonfragmentation amplitude in (14), we readily derive the interference part of the differential cross section. At leading-twist accuracy, the interference term becomes nonvanishing only for the helicity configurations $(\lambda_1, \lambda_2) = (\pm, \mp)$ and (0,0):

$$\frac{d\sigma^{\rm int}_{\pm1,\mp1}}{d\cos\theta} = -\frac{4\pi^3\alpha^4\kappa_{V_1V_2}\mathcal{Q}_{V_1}\mathcal{Q}_{V_2}f_{V_1}f_{V_2}f_{V_1\perp}f_{V_2\perp}}{3r_{V_1}r_{V_2}s^3} \times \lambda^{1/2}(1, r_{V_1}^2, r_{V_2}^2)(3+\cos2\theta)G_{\pm1,\mp1}(\cos\theta), \quad (30a)$$

$$\frac{d\sigma^{\rm int}_{0,0}}{d\cos\theta} = -\frac{32\pi^3\alpha^4\kappa_{V_1V_2}\mathcal{Q}_{V_1}\mathcal{Q}_{V_2}f_{V_1}^2f_{V_2}^2}{3s^3} \times \lambda^{1/2}(1, r_{V_1}^2, r_{V_2}^2)G_{0,0}(\cos\theta), \quad (30b)$$

which bear the following asymptotical behaviors in the limit $\sqrt{s}\to\infty$:

$$\frac{d\sigma^{\rm int}_{\pm1,\mp1,}}{d\cos\theta} \sim \frac{\alpha^4\Lambda_{\rm QCD}^2}{s^2}, \qquad \frac{d\sigma^{\rm int}_{0,0}}{d\cos\theta} \sim \frac{\alpha^4\Lambda_{\rm QCD}^4}{s^3}. \quad (31)$$

Therefore the dominant interference contribution is suppressed with respect to the dominant fragmentation contribution by a factor of $\Lambda_{\rm QCD}^2/s$.

3. Nonfragmentation part

Squaring the nonfragmentation amplitude in (14), and averaging over the electron and positron spins, we then obtain the nonfragmentation part of the differential cross section. For the same reason as in the interference part, at the leading twist accuracy, the nonfragmentation part survives only for the helicity configurations $(\lambda_1, \lambda_2) = (\pm, \mp), (0, 0)$:

$$\frac{d\sigma^{\rm nf}_{\pm1,\mp1}}{d\cos\theta} = \frac{\pi^3\alpha^4\kappa_{V_1V_2}^2f_{V_1\perp}^2f_{V_2\perp}^2}{18s^3}\sin^2\theta(3+\cos2\theta)\lambda^{1/2} \times (1, r_{V_1}^2, r_{V_2}^2)|G_{\pm1,\mp1}(\cos\theta)|^2, \quad (32a)$$

$$\frac{d\sigma^{\rm nf}_{0,0}}{d\cos\theta} = \frac{\pi^3\alpha^4\kappa_{V_1V_2}^2f_{V_1}^2f_{V_2}^2}{9s^3}\lambda^{1/2}(1, r_{V_1}^2, r_{V_2}^2) \times \sin^2\theta|G_{0,0}(\cos\theta)|^2, \quad (32b)$$

which possess the same asymptotical behaviors in the high energy limit:

$$\frac{d\sigma^{\rm nf}_{\pm1,\mp1,}}{d\cos\theta} \sim \frac{\alpha^4\Lambda_{\rm QCD}^4}{s^3}, \qquad \frac{d\sigma^{\rm nf}_{0,0}}{d\cos\theta} \sim \frac{\alpha^4\Lambda_{\rm QCD}^4}{s^3}. \quad (33)$$

Therefore the nonfragmentation part is suppressed with respect to the fragmentation contribution by a factor of $(\Lambda_{\rm QCD}/s)^2$.

B. Production rates for double neutral pseudoscalar mesons

Since the exclusive production of a pair of neutral pseudoscalar pairs only proceeds through the nonfragmentation mechanism, the step of deriving the corresponding differential cross section is identical to Sec. IV A 3. Squaring the nonfragmentation amplitude in (19), and averaging over the electron and positron spins, we obtain

$$\frac{d\sigma^{\rm nf}}{d\cos\theta} = \frac{\pi^3\alpha^4\kappa_{P_1P_2}^2f_{P_1}^2f_{P_2}^2}{9s^3}\lambda^{1/2}(1, r_{V_1}^2, r_{V_2}^2) \times \sin^2\theta|G_{P,P}(\cos\theta)|^2. \quad (34)$$

As mentioned before, the differential cross section for double pseudoscalar meson production very much resembles the nonfragmentation part of the cross section for producing two longitudinally polarized vector mesons, (32b), which also scales as $\alpha^4\Lambda_{\rm QCD}^4/s^3$ in the limit $\sqrt{s}\to\infty$. This asymptotical scaling behavior is the same as that in the $\gamma\gamma\to\pi\pi$ process [21].

V. PHENOMENOLOGY

In this section, we present our predictions for the cross sections of various $e^+e^-\to M_1^0M_2^0$ channels ($M = V, P$). We consider two benchmark values of the e^+e^- center-of-mass energy, $\sqrt{s} = 3.77$ GeV for BESIII experiment, and $\sqrt{s} = 10.58$ GeV for Belle experiment.

A. Input parameters

Our numerical predictions critically hinges on the profile of the LCDAs of various mesons, which must be determined by the nonperturbative means. As a common practice, one parameterizes the meson LCDA as the sum of Gegenbauer polynomials:

TABLE II. Masses, decay constants and a few lower-order Gegenbauer moments of the vector and pseudoscalar mesons.

Vector	ρ	ω	ϕ
Mass [MeV] [37]	775.26	782.66	1019.46
f_V [MeV]	214.7 ± 1.1	195.2 ± 2.9	221.5 ± 1.2
$f_\perp$ [MeV]	165 ± 9 [36]	151 ± 9 [36]	186 ± 9 [36]
$a_1^{\parallel(\perp)}$ ($\mu = 2$ GeV)	0	0	0
$a_2^{\parallel}$ ($\mu = 2$ GeV)	0.132 ± 0.027 [32]	0.132 ± 0.027 [32]	0.13 ± 0.06 [36]
$a_2^{\perp}$ ($\mu = 2$ GeV)	0.101 ± 0.022 [32]	0.101 ± 0.022 [32]	0.11 ± 0.05 [36]

Pseudoscalar	π^0	K^0	η_q	η_s
Mass [MeV] [37]	134.98	497.61	56.81	707.01
f_P [MeV]	130.2 ± 0.12 [37]	155.7 ± 0.3 [37]	125 ± 5 [31]	178 ± 4 [31]
a_1 ($\mu = 2$ GeV)	0	-0.108 ± 0.053 [34]	0	0
a_2 ($\mu = 2$ GeV)	0.116^{+19}_{-20} [33]	0.170 ± 0.046 [34]	0.116^{+19}_{-20} [33]	0.116^{+19}_{-20} [33]
a_3 ($\mu = 2$ GeV)	0	-0.043 ± 0.023 [34]	0	0
a_4 ($\mu = 2$ GeV)	0.122 ± 0.056 [34]	0.073 ± 0.022 [34]	0.122 ± 0.056 [34]	0.122 ± 0.056 [34]
a_6 ($\mu = 2$ GeV)	0.068 ± 0.038 [34]		0.068 ± 0.038 [34]	0.068 ± 0.038 [34]

$$\phi(x) = 6x\bar{x}\left[1 + \sum_{n=1}^{\infty} a_n C_n^{3/2}(2x-1)\right], \qquad (35)$$

with a_n representing the nth Gegenbauer moment.

There have been extensive endeavors to unravel the LCDAs of the ground state mesons from different kinds of phenomenological approaches. In recent years considerable progress has also been made on model-independent extractions of the LCDAs from the lattice QCD simulation. RQCD collaboration has determined the $a_{2\parallel}$ and $a_{2\perp}$ moments for ρ [32], as well as the a_2 moment for the π [33]. The LPC collaboration has also predicted the whole profile of the pion and kaon LCDAs, from which various Gegenbauer moments can be inferred [34]. A very recent two-loop QCD analysis indicates that, taking the RQCD value of a_2, and the LPC values of a_4 and a_6 can give a decent account for both the timelike and spacelike pion electromagnetic form factor data with large momentum transfer [7]. We will adopt the same strategy for the pion LCDA in the phenomenological analysis. Due to the lack of lattice simulation, we assume that the LCDAs of the η_q and η_s are identical to that of the pion, yet differ in decay constants and masses [29,35]. We take the values of

TABLE III. Unpolarized cross sections for $e^+e^- \to V_1^0 V_2^0$ at the benchmark BESIII and Belle energies. For each channel, we also enumerate the individual values of the fragmentation, interference and the nonfragmentation parts.

	$\sqrt{s} = 3.77$ GeV			
Process	$\sigma^{\rm fr}$ [fb]	$\sigma^{\rm int}$ [fb]	$\sigma^{\rm nfr}$ [fb]	$\sigma^{\rm tot}$ [fb]
$e^+e^- \to \rho^0\rho^0$	622 ± 13	-66 ± 8	3.2 ± 0.6	560 ± 15
$e^+e^- \to \rho^0\omega$	111.8 ± 3.5	-36.1 ± 3.4	5.3 ± 0.7	71 ± 5
$e^+e^- \to \rho^0\phi$	152.3 ± 2.3			152.3 ± 2.3
$e^+e^- \to \phi\phi$	9.85 ± 0.21	-4.4 ± 0.7	0.74 ± 0.13	6.2 ± 0.7
$e^+e^- \to \omega\phi$	13.7 ± 0.4			13.7 ± 0.4
$e^+e^- \to \omega\omega$	5.02 ± 0.30	-5.0 ± 0.7	2.2 ± 0.4	2.3 ± 0.8
	$\sqrt{s} = 10.58$ GeV			
Process	$\sigma^{\rm fr}$ [fb]	$\sigma^{\rm int}$ [fb]	$\sigma^{\rm nfr}$ [fb]	$\sigma^{\rm tot}$ [fb]
$e^+e^- \to \rho^0\rho^0$	143.2 ± 2.9	-1.17 ± 0.14	0.007 ± 0.002	142.0 ± 2.9
$e^+e^- \to \rho^0\omega$	25.7 ± 0.8	-0.66 ± 0.06	0.012 ± 0.002	25.1 ± 0.8
$e^+e^- \to \rho^0\phi$	36.1 ± 0.5			36.1 ± 0.5
$e^+e^- \to \phi\phi$	2.36 ± 0.05	-0.08 ± 0.01	0.002 ± 0.0003	2.27 ± 0.05
$e^+e^- \to \omega\phi$	3.25 ± 0.10			3.25 ± 0.10
$e^+e^- \to \omega\omega$	1.16 ± 0.07	-0.09 ± 0.01	0.005 ± 0.001	1.07 ± 0.07

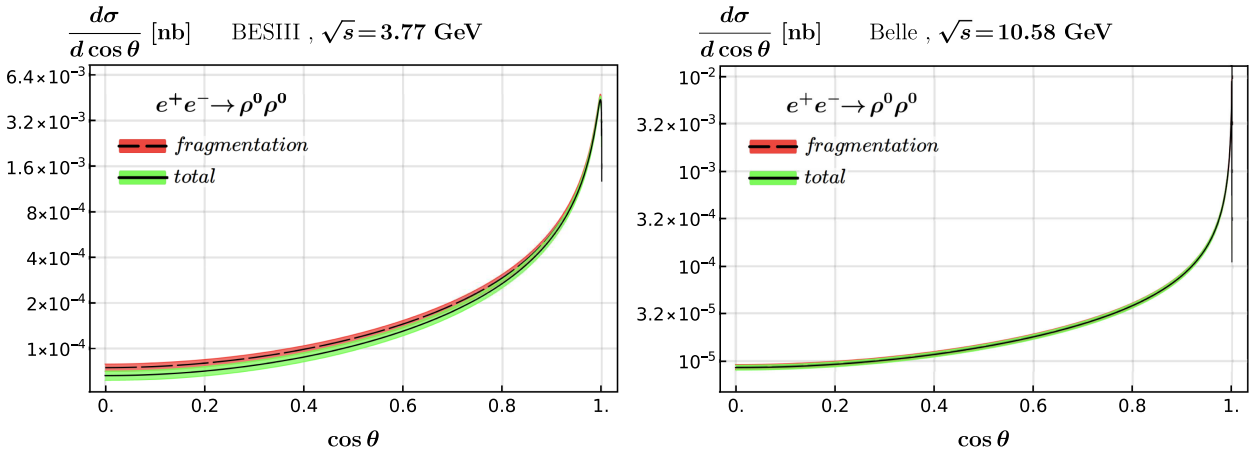

FIG. 2. The angular distribution of the ρ^0 in the process $e^+e^-\to\rho^0\rho^0$. The red band represents the contribution from fragmentation mechanism only, while the green band represents the sum of the fragmentation, interference, and nonfragmentation contributions.

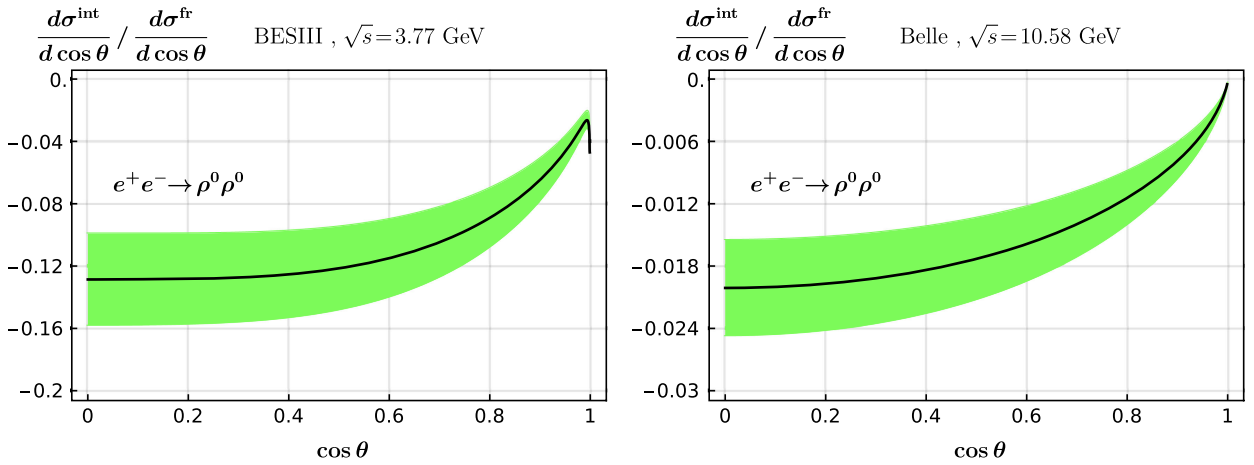

FIG. 3. The ratio of the interference part to the fragmentation part in the process $e^+e^-\to\rho^0\rho^0$ as a function of $\cos\theta$.

the first four Gegenbauer moments of the K^0 meson as given by LPC [34]. In the absence of the lattice result, we assume the Gegenbauer moments of ω is identical to those of ρ, and take the moments of the ϕ meson from QCD sum rules analysis [36].

In addition, we take the values of the π and K^0 decay constants from the latest compilation of PDG [37], and take the lattice predictions of η_q and η_s decay constants given by the ETM collaboration [31]. We fix the values of the decay constants f_V for $(V=\rho,\omega,\phi)$ from the measured leptonic widths [37], and take the values of the decay constants $f_{V\perp}$ from the QCD sum rules analysis [36].

For reader's convenience, in Table II we enumerate the values of the mass, decay constant and a few first Gegenbauer moments of light neutral vector and pseudoscalar mesons.

In our numerical calculation, we choose to use the QED coupling constant $\alpha(\sqrt{s}/2)=1/133.46$ for BESIII and $\alpha(\sqrt{s}/2)=1/132.02$ for Belle experiment. These values of the running QED couplings are evaluated by utilizing the package PYTHIA [38].

B. Numerical results

In Table III we enumerate the cross sections for various exclusive double vector meson and double pseudoscalar production channels, both at BESIII and Belle energies. For the case when the two vector mesons are identical particles, we have to integrate the differential cross section over only half of the entire phase space.

The total cross sections of three channels $e^+e^-\to\rho^0\rho^0,\rho^0\omega,\rho^0\phi$ at $\sqrt{s}=3.77$ GeV are predicted to be 560 ± 15, 71 ± 5, and 152.3 ± 2.3 fb, respectively. To date the BESIII experiment has accumulated about 20 fb^{-1} data at this energy point, so there have already been 10900–11500, 1320–1520 and 3000–3092 events

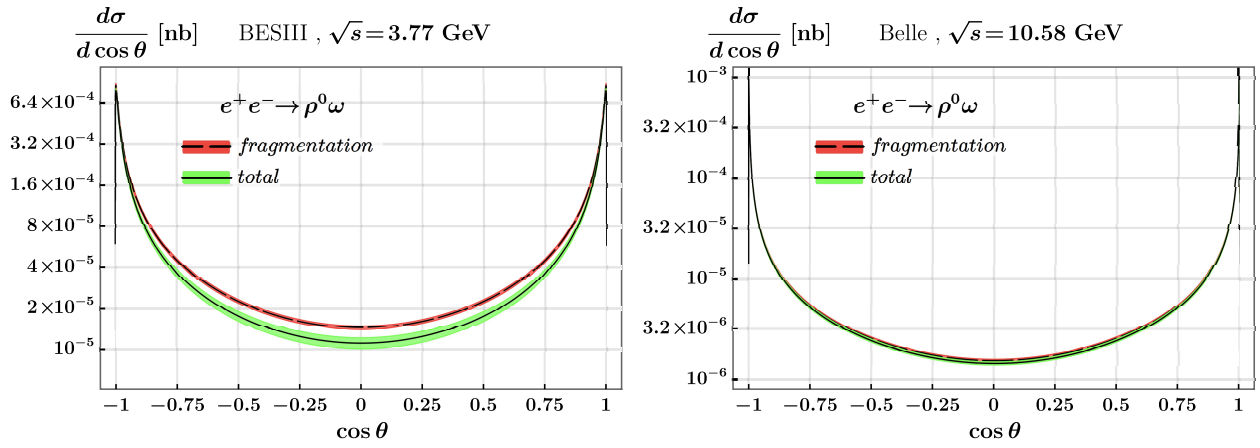

FIG. 4. The angular distribution of the ρ^0 in the process $e^+e^-\to\rho^0\omega$. The red band represents the fragmentation contribution, while the green band represents the sum of three pieces of contributions.

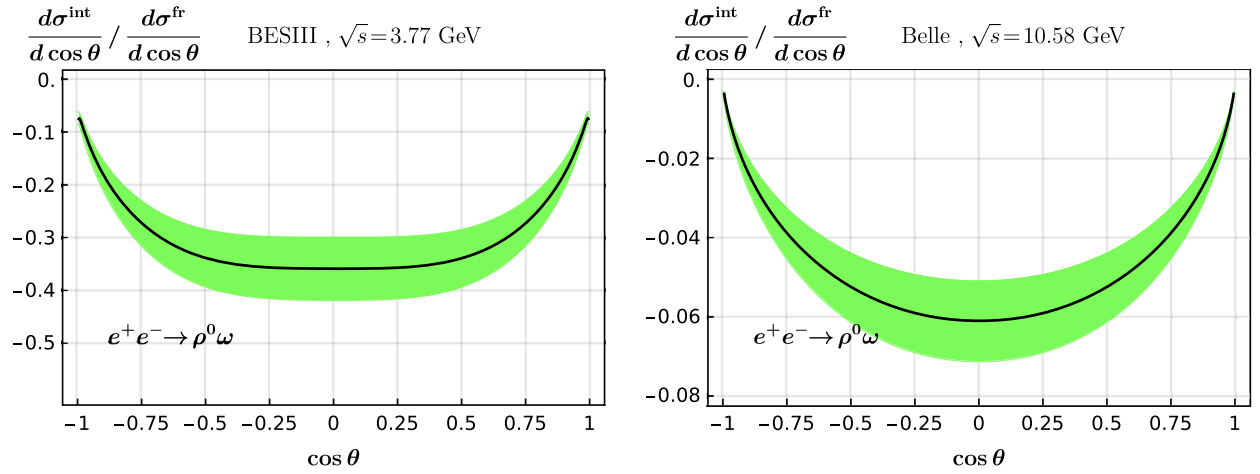

FIG. 5. The angular distribution of the ratio of the interference part to the fragmentation part in the process $e^+e^-\to\rho^0\omega^0$.

produced. Therefore, these three channels should be readily observed based on current BESIII dataset.

In contrast, the total production rates of the three processes $e^+e^+\to\rho^0\rho^0,\rho^0\omega,\rho^0\phi$ at $\sqrt{s}=10.58$ GeV are predicted to be 142.0 ± 2.9, 25.1 ± 0.8, and 36.1 ± 0.5 fb, respectively. The cross sections are more than three times smaller than those at BESIII, which is compatible with the asymptotic scaling behavior $\sigma^{\rm fr}(\sqrt{s})\sim\alpha^4/s$ in (27a), since the double neutral vector meson production is dominated by the fragmentation mechanism at high energy.

Thus far the integrated luminosity of Belle experiment has reached about 1500 fb^{-1}, and we expect about 208650–217350 $\rho^0\rho^0$ events, 36450–38850 $\rho^0\omega$ events, and 53400–54900 $\rho^0\phi$ events have been produced. These double vector meson events are so copious and deserve a dedicated study experimentally.

Equation (28) indicates that the fragmentation contributions to the three production channels obey the hierarchy: $\sigma(\rho^0\rho^0):\sigma(\rho^0\omega):\sigma(\rho^0\phi)\approx\mathcal{Q}_\rho^2/2:\mathcal{Q}_\omega^2:\mathcal{Q}_\phi^2=9:2:4$, where the effective quark electric charge in a vector meson given in (6).[6] We clearly see from Table III that the predicted cross

TABLE IV. Total cross sections for $e^+e^-\to P_1^0P_2^0$ at BESIII and Belle energies.

	BESIII, $\sigma^{\rm tot}$ [ab]	Belle, $\sigma^{\rm tot}$ [ab]
$e^+e^-\to\pi^0\pi^0$	444 ± 212	1.0 ± 0.5
$e^+e^-\to\pi^0\eta$	175 ± 85	0.38 ± 0.5
$e^+e^-\to\pi^0\eta'$	108 ± 53	0.25 ± 0.12
$e^+e^-\to\eta\eta$	310 ± 152	0.69 ± 0.34
$e^+e^-\to\eta'\eta'$	255 ± 124	0.62 ± 0.30
$e^+e^-\to\eta\eta'$	2.9 ± 3.1	0.007 ± 0.007
$e^+e^-\to K_S^0K_S^0$	121 ± 35	0.27 ± 0.08

[6]Owing to the smaller effective quark charge in ω and ϕ relative to that in ρ^0, the production rates for $e^+e^-\to\phi\phi,\phi\omega,\omega\omega$ are orders of magnitude suppressed with respect to those for $e^+e^-\to\rho^0\rho^0,\rho^0\omega,\rho^0\phi$.

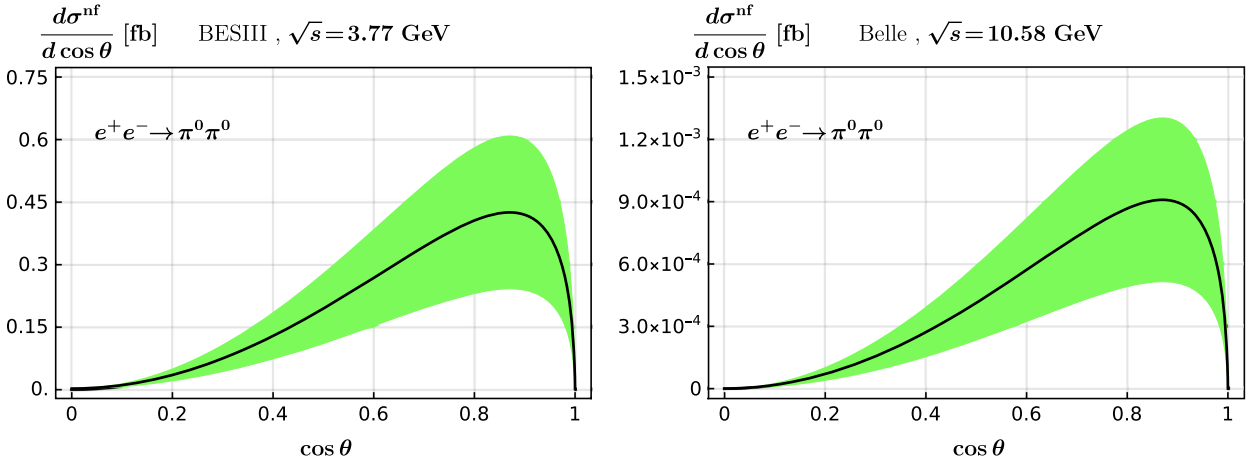

FIG. 6. Angular distribution of the π^0 in the $e^+e^-\to\pi^0+\pi^0$ process.

sections at Belle fit into this pattern better than those at BESIII, since the fragmentation dominance is a much better approximation in the higher energy e^+e^- collider.

In addition to the total cross section, in Table III we also enumerate the individual contribution from the fragmentation, interference and nonfragmentation parts for a variety of double vector meson production channels. One clearly sees that the interference contributions are destructive. For the Belle, the magnitude of the interference piece is smaller than the uncertainty of the fragmentation contribution. Since the estimated fragmentation contribution [10,11] already successfully accounts for the measured production rates of the $e^+e^-\to\rho^0\rho^0$ and $\rho^0\phi$ processes by *BABAR* [9], it seems unfeasible to unambiguously pinpoint the interference contribution from the experimental perspective, even with a great amount of events at Belle experiment.

As can be clearly visualized in Table III, it turns out that the interference effect is much more significant at BESIII experiment. For the $e^+e^-\to\rho^0\rho^0$ channel, including the interference contribution can lower the fragmentation prediction by about 10%; For the $e^+e^-\to\rho^0\omega$ channel, including the interference contribution may even lower the fragmentation contribution by 30%. It is easy to understand why the interference contribution becomes notable at BESIII but negligible at Belle, since the interference contribution is suppressed with respect to the fragmentation contribution by a factor of $\Lambda^2_{\rm QCD}/s$, as indicated by (27a) and (31).

The impact of the interference contribution for $e^+e^-\to\rho^0\rho^0$ can also been seen in the angular distribution of ρ^0 in Figs. 2 and 3. Clearly, the interference effect in this channel becomes already notable at BESIII experiment. More interestingly, as can be seen from the angular distribution of the ρ^0 meson in Figs. 4 and 5, the impact of the interference contribution the for $e^+e^-\to\rho^0\omega$ channel becomes significant at BESIII energy.

We also observe from Table III that, the nonfragmentation contribution in various double vector meson production processes, which receive a $\Lambda^4_{\rm QCD}/s^2$ suppression with respect to the fragmentation prediction, become completely negligible, even at BESIII energy.[7]

We thus urge the future BESIII experiment to conduct a precise measurement of the differential cross sections for the $e^+e^-\to\rho^0\rho^0$ and $e^+e^-\to\rho^0\omega$ channels. Once the definite deviation from the fragmentation prediction is observed, one may unambiguously establish the existence of the destructive interference contribution. By confronting theoretical predictions and experimental measurements, our knowledge about the LCDAs of ρ^0 and ω will be greatly enhanced.

In Table IV we also enumerate the cross sections for various exclusive double neutral pseudoscalar meson production channels, both at BESIII and Belle energies. The production rates turn out to be exceedingly tiny, which reach only a few tenth of fb for the $e^+e^-\to\pi^0\pi^0,\eta\eta,\eta'\eta',\pi^0\eta$ channels at $\sqrt{s}=3.77$ GeV. For concreteness, we plot the angular distribution of the π^0 for the $e^+e^-\to\pi^0+\pi^0$ process in Fig. 6. The smallness of the cross sections is clearly rooted in the $\alpha^4\Lambda^4_{\rm QCD}/s^3$ scaling behavior dictated by the nonfragmentation mechanism. It looks rather challenging to observe these rare exclusive production channels at BESIII experiment.

VI. SUMMARY

In this work, we have conducted a comprehensive investigation on the exclusive production of double light neutral mesons (with $C=+1$) from e^+e^- annihilation, exemplified by the BESIII and Belle experiments. These exclusive processes necessarily entail two-photon

[7]An exception is the $e^+e^-\to\omega\omega$ channel at BESIII energy, where the fragmentation and interference pieces coincidentally nearly cancel with each other, so the nonfragmentation contribution becomes the dominant one.

exchange, with the double neutral meson production mechanism classified into the photon fragmentation and nonfragmentation. The fragmentation contribution is only relevant for double neutral vector meson production, which can be reliably estimated in a rigorous manner, by taking the measured leptonic width of the neutral vector meson as input. The nonfragmentation amplitudes are computed within the framework of collinear factorization, to the lowest order in QED and QCD coupling and at leading twist accuracy.

For the exclusive production of a pair of light neutral pseudoscalar mesons, only the nonfragmentation production mechanism survives, and the corresponding production rates are too small for these types of processes to be observed at both BESIII and Belle. The exclusive production of a pair of light neutral vector mesons is more interesting. The cross sections are generally quite large owning to the kinematic enhancement brought by the fragmentation mechanism, so that such processes should be readily observed and precisely measured in both BESIII and Belle experiments. Although the fragmentation contribution plays the dominant role, including the nonfragmentation contribution may bring in a sizable destructive interference effect at BESIII energy. We find that, with certain choice of the ρ^0/ω LCDAs inspired by the lattice QCD study, including the interference effect may lower the fragmentation contribution to the production rate for $e^+e^- \to \rho^0\rho^0$ at $\sqrt{s} = 3.77$ GeV by about 10%, and decrease the fragmentation prediction for $e^+e^- \to \rho^0\omega$ by about 30%. Thanks to a copious number of $\rho^0\rho^0$ and $\rho^0\omega$ events produced in the BESIII experiment, it is feasible to accurately measure the angular distributions of these processes. Observation of explicit deviation from the fragmentation predictions will unambiguously indicate the existence of the interference effect. Confronting the future BESIII measurements with our predictions, it seems possible to impose useful constraints on the profile of the ρ^0/ω LCDAs. The new knowledge gleaned from the double vector meson production at BESIII may in turn be beneficial to precise predictions of $B \to V$ form factor and $B \to VV$ decay rates.

ACKNOWLEDGMENTS

We thank Deshan Yang for discussions. The work of C.-P. J., Y. J. and J.-L. L is supported in part by the National Natural Science Foundation of China under Grant No. 11925506. The work of X.-N. X. is supported in part by the National Natural Science Foundation of China under Grant No. 12275364.

[1] T. K. Pedlar *et al.* (CLEO Collaboration), Phys. Rev. Lett. **95**, 261803 (2005).
[2] B. Aubert *et al.* (*BABAR* Collaboration), Phys. Rev. D **78**, 071103 (2008).
[3] G. P. Lepage and S. J. Brodsky, Phys. Lett. **87B**, 359 (1979).
[4] R. D. Field, R. Gupta, S. Otto, and L. Chang, Nucl. Phys. **B186**, 429 (1981).
[5] A. B. Arbuzov, V. A. Astakhov, A. V. Fedorov, G. V. Fedotovich, E. A. Kuraev, and N. P. Merenkov, J. High Energy Phys. 10 (1997) 006.
[6] Z. Lu and I. Schmidt, Phys. Rev. D **73**, 094021 (2006); **75**, 099902(E) (2007).
[7] L. B. Chen, W. Chen, F. Feng, and Y. Jia, arXiv:2312.17228.
[8] N. A. Kivel and M. V. Polyakov, J. High Energy Phys. 11 (2009) 072.
[9] B. Aubert *et al.* (*BABAR* Collaboration), Phys. Rev. Lett. **97**, 112002 (2006).
[10] M. Davier, M. E. Peskin, and A. Snyder, arXiv:hep-ph/0606155.
[11] G. T. Bodwin, E. Braaten, J. Lee, and C. Yu, Phys. Rev. D **74**, 074014 (2006).
[12] B. Gong and J. X. Wang, Phys. Rev. Lett. **100**, 181803 (2008).
[13] W. L. Sang, F. Feng, Y. Jia, Z. Mo, J. Pan, and J. Y. Zhang, Phys. Rev. Lett. **131**, 161904 (2023).
[14] X. D. Huang, B. Gong, R. C. Niu, H. M. Yu, and J. X. Wang, J. High Energy Phys. 02 (2024) 055.
[15] G. T. Bodwin, E. Braaten, and G. P. Lepage, Phys. Rev. D **51**, 1125 (1995); **55**, 5853(E) (1997).
[16] G. P. Lepage and S. J. Brodsky, Phys. Rev. D **22**, 2157 (1980).
[17] V. L. Chernyak and A. R. Zhitnitsky, Phys. Rep. **112**, 173 (1984).
[18] K. Abe *et al.* (Belle Collaboration), Eur. Phys. J. C **32**, 323 (2003).
[19] H. Nakazawa *et al.* (Belle Collaboration), Phys. Lett. B **615**, 39 (2005).
[20] T. Mori *et al.* (Belle Collaboration), J. Phys. Soc. Jpn. **76**, 074102 (2007).
[21] S. J. Brodsky and G. P. Lepage, Phys. Rev. D **24**, 1808 (1981).
[22] M. Benayoun and V. L. Chernyak, Nucl. Phys. **B329**, 285 (1990).
[23] V. L. Chernyak, Nucl. Phys. B, Proc. Suppl. **162**, 161 (2006).
[24] V. L. Chernyak, Phys. Lett. B **640**, 246 (2006).
[25] V. L. Chernyak and S. I. Eidelman, Prog. Part. Nucl. Phys. **80**, 1 (2015).
[26] M. Klusek, W. Schafer, and A. Szczurek, Phys. Lett. B **674**, 92 (2009).
[27] J. J. Sakurai, Ann. Phys. (N.Y.) **11**, 1 (1960).

[28] M. Beneke and T. Feldmann, Nucl. Phys. **B592**, 3 (2001).
[29] T. Feldmann, P. Kroll, and B. Stech, Phys. Rev. D **58**, 114006 (1998).
[30] H. Y. Cheng, H. n. Li, and K. F. Liu, Phys. Rev. D **79**, 014024 (2009).
[31] K. Ottnad *et al.* (ETM Collaboration), Phys. Rev. D **97**, 054508 (2018).
[32] V. M. Braun, P. C. Bruns, S. Collins, J. A. Gracey, M. Gruber, M. Göckeler, F. Hutzler, P. Pérez-Rubio, A. Schäfer, W. Söldner *et al.*, J. High Energy Phys. 04 (2017) 082.
[33] G. S. Bali *et al.* (RQCD Collaboration), J. High Energy Phys. 08 (2019) 065.
[34] J. Hua *et al.* (Lattice Parton Collaboration), Phys. Rev. Lett. **129**, 132001 (2022).
[35] A. Ali, G. Kramer, Y. Li, C. D. Lu, Y. L. Shen, W. Wang, and Y. M. Wang, Phys. Rev. D **76**, 074018 (2007).
[36] P. Ball and G. W. Jones, J. High Energy Phys. 03 (2007) 069.
[37] R. L. Workman *et al.* (Particle Data Group), Prog. Theor. Exp. Phys. **2022**, 083C01 (2022).
[38] C. Bierlich, S. Chakraborty, N. Desai, L. Gellersen, I. Helenius, P. Ilten, L. Lönnblad, S. Mrenna, S. Prestel, C. T. Preuss *et al.*, SciPost Phys. Codebases **2022**, 8 (2022).